Coastal-Ocean Processes and their Influence on the Oil Spilled off San Francisco by the M/V *Puerto Rican*†

Laurence C. Breaker

NOAA National Meteorological Center, Washington, DC, 20233, USA

&

Alan Bratkovich*

NOAA Great Lakes Environmental Research Laboratory,
Ann Arbor, Michigan 48105, USA

ABSTRACT

The oil tanker M/V Puerto Rican *exploded on 31 October 1984 and later broke apart to produce a major oil spill in the coastal waters off San Francisco, California, USA. Oil from this spill initially moved to the SSW until 5 November, when it abruptly reversed direction and began moving rapidly to the north and then to the NNW during the following week.*

The oceanic processes that most likely contributed to the displacement of the oil spilled by the Puerto Rican *are examined within the framework of a simple, empirical-hindcasting model. A large-scale flow component, wind drift, and tidal currents are included in the model. Wind drift, inferred by using a simple linear formulation, was the single most important factor in determining the over-all displacement of the oil. Residuals from the model, however, indicate that the winds alone could not fully account for the sudden and dramatic reversal in oil movement that occurred on 5 November 1984. This reversal was surge-like and coincided with an increase in sea level along the central California coast. Finally, the close agreement between the local and advective changes in sea-surface temperature in the Gulf of the Farallones at the time of the* Puerto Rican *oil spill indicate, although not conclusively, that this reversal could have been related to the onset of the Davidson Current or other larger-scale flow phenomena.*

* Also at: Department of Atmospheric, Oceanic and Space Sciences, University of Michigan, Ann Arbor, Michigan 48109, USA.
† OPC Contribution No. 67.

INTRODUCTION

On 31 October 1984, the oil tanker M/V *Puerto Rican* exploded about 30 km west of the Golden Gate Bridge, San Francisco (Fig. 1). Three days later, the *Puerto Rican* broke in two while under two. The stern section sank and produced a major oil spill in the Gulf of the Farallones. An estimated 1·5 million gallons of oil were spilled into the ocean as a result of this accident (Herz & Kopec, 1985). The resulting spill gradually spread south over the next three days. However, on 5 November, the oil-spill
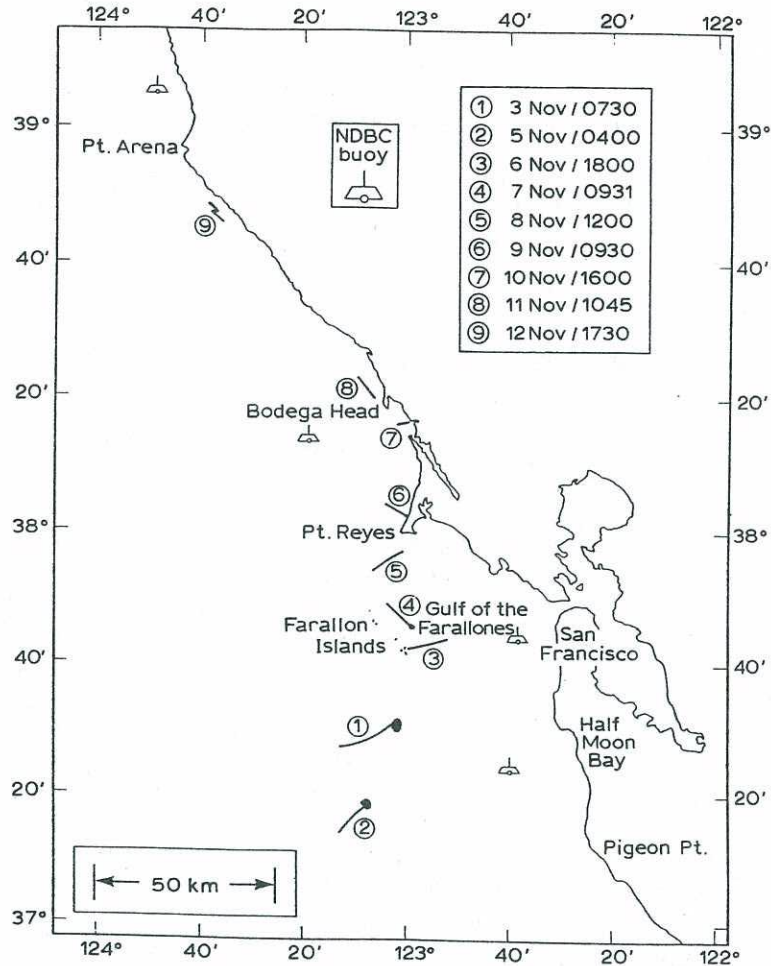

Fig. 1.   Oil-slick locations at different times along the central California coast during the period of the *Puerto Rican* tanker oil spill between 3 and 12 November 1984. Approximate shapes of the oil-slick pattern are also indicated; hence the bulbous extremities associated with the oil slicks at locations 1 and 2.

N

Puerto Rican exploded about
Francisco (Fig. 1). Three days
under two. The stern section
Gulf of the Farallones. An
d into the ocean as a result of
sulting spill gradually spread
on 5 November, the oil-spill

3 Nov / 0730	
5 Nov / 0400	
6 Nov / 1800	
7 Nov / 0931	
8 Nov / 1200	
9 Nov / 0930	
10 Nov / 1600	
11 Nov / 1045	
12 Nov / 1730	

ntral California coast during the
12 November 1984. Approximate
ie bulbous extremities associated
nd 2.

trajectory suddenly reversed direction. By 6 November, oil was observed around the Farallon Islands, approximately 50 km north of its location on the previous day. Over the next seven days, oil from the spill was observed along the coast as far north as Pt Arena. Oil also came ashore at several locations around Pt Reyes and further north near Bodega Head. Although the over-all impact on the local marine environment was not considered severe, it was estimated that there were as many as 5000 bird mortalities that resulted from this spill.

Various oceanic processes undoubtedly contributed to the advection and dispersion of the oil spilled by the *Puerto Rican*. This spill episode is relatively unique in that slick-trajectory information is unusually detailed, and the trajectory itself passed through a region that contains an array of four National Data Buoy Center (NDBC) meteorological buoys (at least one buoy was always within 50 km of the spill). Moreover, extensive historical literature on the physical oceanography of this region exists. This information is used to examine and prioritize the importance of the various oceanic processes that influenced the path followed by the oil during its passage through the Gulf of the Farallones and further north along the California coast.

To provide a framework for this study, we employ a simple, empirical model to hindcast the oil-spill trajectory. We also consider the likelihood that the onset of the Davidson Current or some other larger-scale flow feature may have contributed to the sudden and dramatic reversal experienced by the oil during its movement through the Gulf. In the subsequent analyses, we refer to this possibility as an apparent current reversal (ACR).

ENVIRONMENTAL SETTING

In this section, we present historical oceanographic data as well as oceanographic data acquired along the central California coast surrounding the period of the *Puerto Rican* oil spill. The historical data include a map of surface dynamic topography (0/500 db) off the California coast for November (Wyllie, 1966; Fig. 2). Poleward flow along the central California coast at least as far north as San Francisco is indicated with an offshore length scale of 100–200 km. The spatially and temporally averaged amplitude of this flow approaches 10 cm s^{-1}.

The data acquired around the period of the oil spill include surface wind, sea-surface temperature (SST), and sea level. Acquisition sites for these data are shown in Fig. 3 and their associated characteristics are given in Table 1.
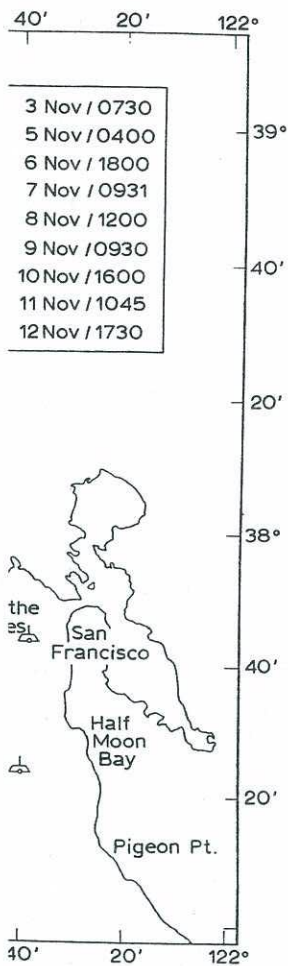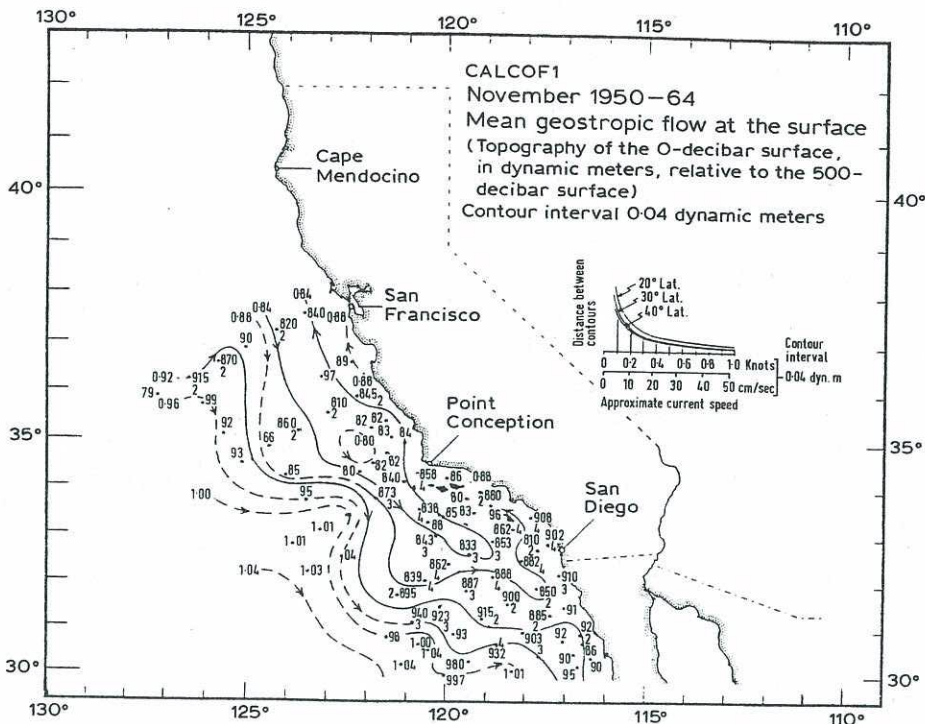
Fig. 2. Mean geostrophic flow at the surface (0/500 db) off California for the period 1950–1964 for November (from Wyllie, 1966).

Surface winds, acquired from NDBC buoys along the California coast, were converted to wind stress according to the equation:
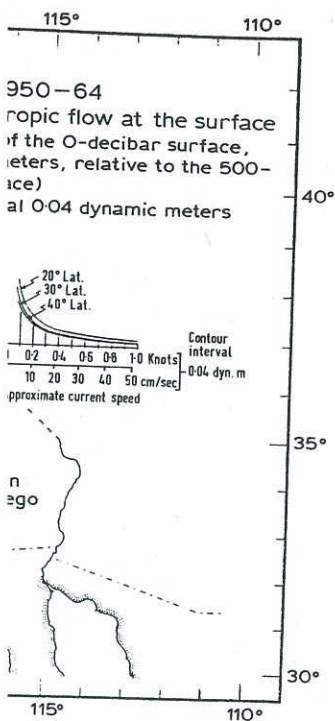
$$\tau = C_d \rho_a \mathbf{U}_{10} |\mathbf{U}_{10}| \qquad (1)$$

where C_d is the drag coefficient, ρ_a is the density of air, and $\mathbf{U}_{10}$ is the wind velocity at 10 m. A constant drag coefficient of $1{\cdot}3 \times 10^{-3}$ was employed. The results are displayed as vector time series or so-called stick diagrams (Fig. 4). Hourly observations of SST from the NDBC buoys are shown in Fig. 5. Hourly sea-level elevations, acquired from National Ocean Service tide gages, were initially smoothed by using a low-pass filter with a half-power cutoff of 40 hours (Godin, 1972). An inverse barometer correction was then applied by using the surface pressure from the nearest NDBC buoy in each case to yield the adjusted sea level (Fig. 6).

Stick diagrams of surface wind stress generally indicate stronger winds to the north at the northern locations between the last week in October

950—64
ropic flow at the surface
of the O-decibar surface,
eters, relative to the 500—
ce)
al 0·04 dynamic meters

20° Lat.
30° Lat.
40° Lat.

Contour
interval
·0·04 dyn. m

0·2 0·4 0·6 0·8 1·0 Knots

10 20 30 40 50 cm/sec

pproximate current speed

) off California for the period
, 1966).

long the California coast,
quation:

$$(1)$$

ty of air, and U_{10} is the
cient of $1\cdot3 \times 10^{-3}$ was
time series or so-called
f SST from the NDBC
evations, acquired from
ly smoothed by using a
ours (Godin, 1972). An
l by using the surface
ase to yield the adjusted

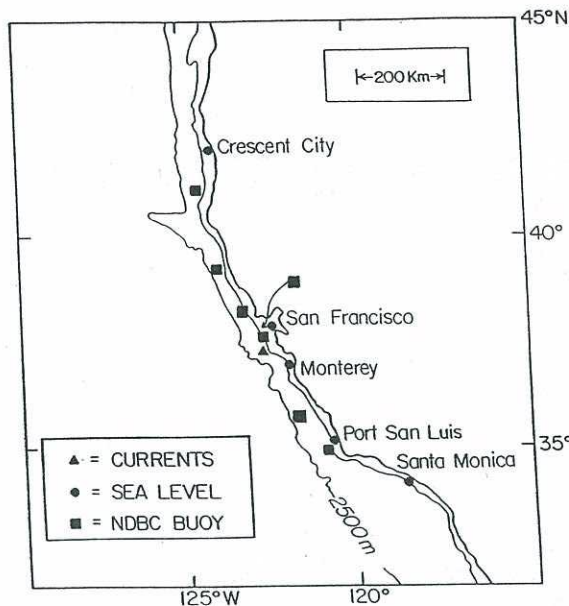indicate stronger winds
he last week in October

Fig. 3. Locator map for sea level and NDBC buoy data. NDBC buoy data include surface winds, sea-surface temperature, and barometric pressure.

and mid-November (Fig. 4). Typical wind-stress amplitudes are approximately 1 dyn cm^{-2}; absolute maxima exceed 6 dyn cm^{-2}. Brief wind events on 2 and 5 November can also be identified in the Gulf of the Farallones (i.e., at 37·4°N and 37·8°N).

SST increased by 2°C or more during the first half of November between 37·4 and 39·2°N (Fig. 5). This period of increasing SSTs starts several days earlier at 39·2°N than it does further south, consistent with the phasing of downwelling-favorable winds, which first develop in the northern portion of the study area and then progress equatorward.

Adjusted sea level generally increases at locations along the California coast from Monterey northward during the first half of November, con-

TABLE 1
The Environmental Data

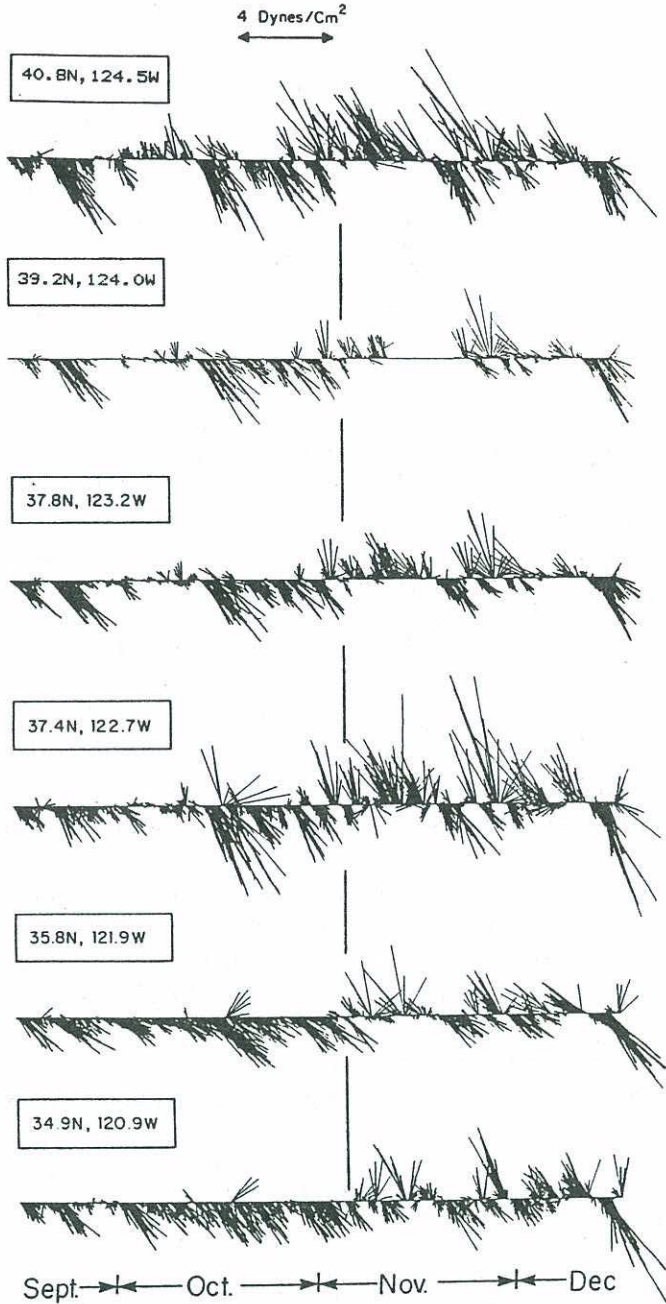| Variable	Height above (+) or depth below (−) sea level	Δt (h)	Duration (1984)
Surface wind	+10 m	1	15 Sept.–15 Dec.
Sea-surface temperature	1 m	1	15 Sept.–15 Dec.
Sea level	0 m	1	15 Sept.–15 Dec.

Fig. 4. Stick diagrams of hourly surface-wind stress at six locations along the California coast. Period covers 15 September–15 December 1984. Sticks pointing toward the top of the page indicate winds to the north, etc. The vertical line that extends across each of the plots coincides with the time of the apparent current reversal that occurred in the Gulf of the Farallones on 5 November 1984.
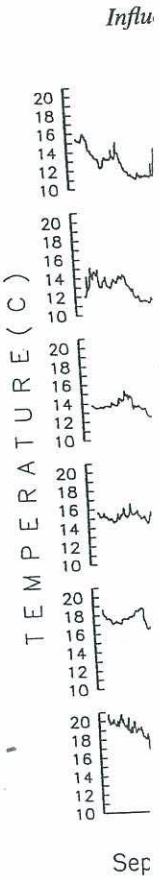
Fig. 5. Hourly adjus
coast from 15 Septem
the plots coincides wi

sistent with the c
increases are not
and into Decemb
amplitude) occur
the first week in
adjusted sea level
    Eighteen temp
Farallones for th
shown in Fig. 7 (
Taking first majc
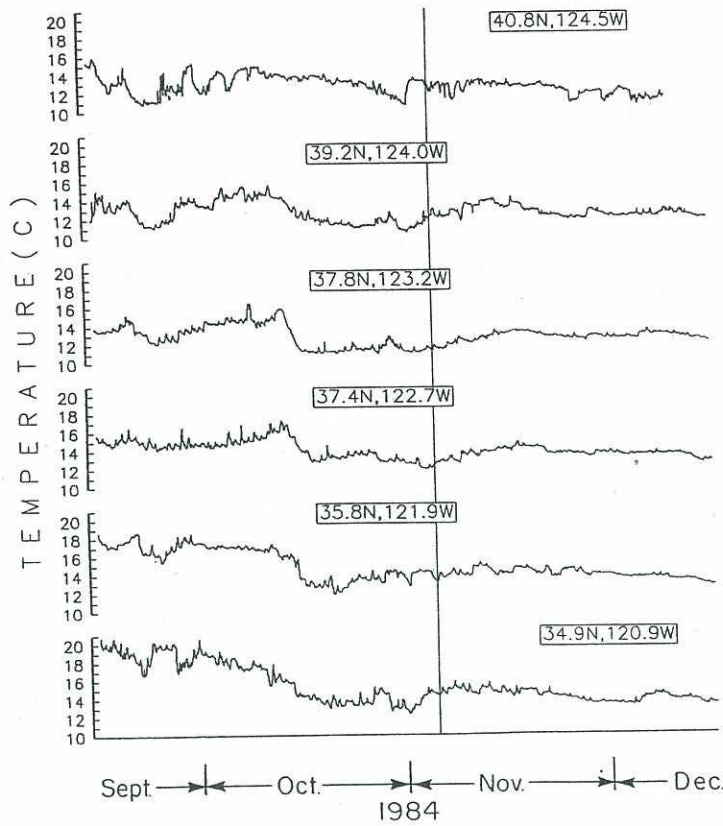the maximum d
mixed-layer dept
    Subsurface cu

Fig. 5. Hourly adjusted sea surface temperatures at six locations along the California coast from 15 September to 15 December. The vertical line that extends across each of the plots coincides with the time of the apparent current reversal that occurred in the Gulf of the Farallones on 5 November 1984.

sistent with the onset of downwelling-favorable winds, although these increases are not as clearly sustained during the latter half of November and into December (Fig. 6). Abrupt increases (approximately 20 cm in amplitude) occur at Monterey, San Francisco, and Crescent City during the first week in November. It is noteworthy that similar increases in adjusted sea level are not observed south of Monterey.

Eighteen temperature profiles acquired in or near the Gulf of the Farallones for the period between 15 October and 19 November 1984 are shown in Fig. 7 (obtained from the National Oceanographic Data Center). Taking first major-inflection points below the surface as an indication of the maximum depth of wind influence (i.e. surface mixed-layer depth), mixed-layer depths ranged from 30 to 60 m.

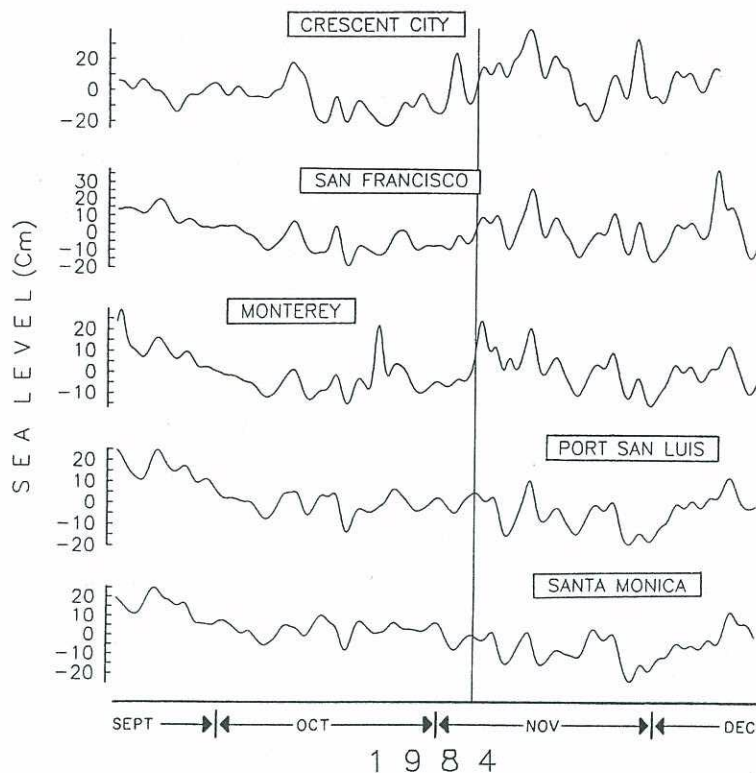Subsurface current-meter data (at a depth of 70 m) were also available

Fig. 6. Hourly sea level at five locations along the California coast from 15 September to 15 December 1984. Sea-level data have been low-pass filtered to suppress the tides and adjusted for variations in barometric pressure. The vertical line that extends across each of the plots coincides with the time of the apparent current reversal that occurred in the Gulf of the Farallones on 5 November 1984.

at several locations along the continental shelf and slope south of San Francisco (Half Moon Bay, 37·5°N, 122·5°W, and Pt Sur, 36·0°N, 122·0°W) during the period of the *Puerto Rican* oil spill. However, on the basis of the temperature profiles acquired in the study area, and the fact that the slick itself never approached closer than 40 km to the nearest moored current-meter site, we conclude (i) that current-meter observations at a depth of 70 m are most likely too deep to be taken as an indicator of surface flow in this region (well below the seasonal thermocline, see Fig. 7), and (ii), the observation sites are most likely too distant to be representative, especially in view of the irregular coastline and bottom topography of the region. Furthermore, subtidal, subsurface current fluctuations have been shown to have horizontal correlation length scales of only a few tens of km in this region (e.g., Winant *et al.*, 1987; Chelton *et al.*, 1988).
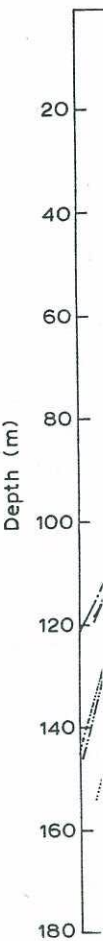
Fig. 7. Eight
Farallones bet

ANALYS

Spill-traject

The oil spi
tracked by

ORT SAN LUIS

NTA MONICA

▶|◀—— DEC

coast from 15 September
to suppress the tides and
that extends across each
reversal that occurred in
1984.

slope south of San
Sur, 36·0°N, 122·0°W)
ever, on the basis of
nd the fact that the
the nearest moored
er observations at a
as an indicator of
rmocline, see Fig. 7),
to be representative,
bottom topography
current fluctuations
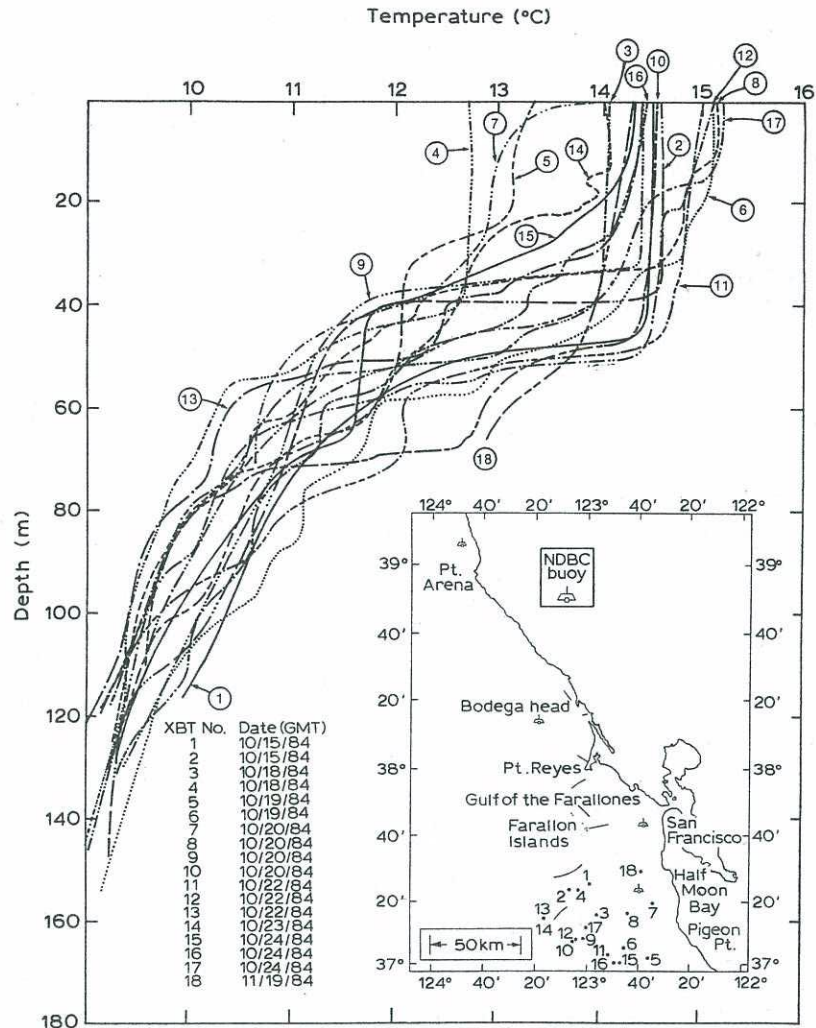ngth scales of only
1987; Chelton *et al.*,

Fig. 7. Eighteen temperature profiles acquired in and adjacent to the Gulf of the Farallones between 15 October 1984 and 19 November 1984 (NODC, 1989). Inset in the lower right-hand corner indicates the location of each profile.

XBT No.	Date (GMT)
1	10/15/84
2	10/15/84
3	10/18/84
4	10/18/84
5	10/19/84
6	10/19/84
7	10/20/84
8	10/20/84
9	10/20/84
10	10/20/84
11	10/22/84
12	10/22/84
13	10/22/84
14	10/23/84
15	10/24/84
16	10/24/84
17	10/24/84
18	11/19/84

ANALYSIS OF THE OIL-SPILL TRAJECTORY AND RELATED PROCESSES

Spill-trajectory analyses

The oil spilled by the *Puerto Rican* in the Gulf of the Farallones was tracked by US Coast Guard aircraft overflights between 31 October and

17 November 1984. During this period, the oil-slick locations and associated patterns were mapped as the oil moved initially southward and then to the north. Figure 1 shows the time history of oil-slick movement from 3 to 12 November 1984. The slick patterns included in this time history are a subset of the total number that were identified and tracked by the Coast Guard. They were selected on the basis of providing the most consistent over-all trajectory for the displaced oil. Slick centroids were determined by estimating the geometric center of the slick at each siting. Displacements were then found by measuring the (rectilinear) distances between the geometric centers at successive slick locations.

The observations are consistent in that (i) they include the same oil type (color) where oil type was identified, (ii) the selected patterns are similar in shape, and (iii), the velocities associated with the oil-slick displacements are of the same order as the current velocities reported previously in this region. The oil patches depicted in Fig. 1 (and most of those not shown) tended to maintain their shape as elongated filaments (approximately 5–18 km in length) as they progressed upcoast. We note that there are many possible sources of error in such observations as the slick evolved over time. We have assumed, however, that any errors in oil-slick location were relatively small.

A progressive vector diagram (PVD) of the oil-slick displacements (Fig. 8(a)) indicates that the oil moved SSW between 3 and 5 November and then to the NNE between 5 and 6 November, after which time it moved to the NW. There is a total displacement of almost 200 km between 3 and 12 November. After this time period (our analysis time window), the slick moved offshore near Pt Arena. The associated average advection speed is approximately 20 cm s^{-1} to the NNW. In addition to the PVD, displacement and Lagrangian-velocity vector time series for the oil-slick movement history have been constructed (see Figs 9(a), 10(a)). Rectilinear motion was assumed throughout. Maximum displacements (approximately 77 km) and speeds (approximately 56 km day^{-1}) occurred on 12 November, when the oil was located near the coast, just south of Pt Arena. Both vector sequences also show the sudden major reversal in oil-slick movement that occurred on 5 November 1984, with an associated displacement and velocity of approximately 62 km and approximately 37 km day^{-1}, respectively. However, because the intervals between oil-slick sitings did not vary appreciably (15–44 hours), the velocity and displacement vector sequences are generally similar. Consequently the displacement vector time series is primarily referred to.
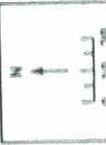
slick locations and
initially southward
history of oil-slick
patterns included in
that were identified
ted on the basis of
or the displaced oil.
geometric center of
found by measuring
centers at successive

include the same oil
selected patterns are
ed with the oil-slick
t velocities reported
n Fig. 1 (and most of
s elongated filaments
ed upcoast. We note
such observations as
ever, that any errors

l-slick displacements
n 3 and 5 November
·, after which time it
t of almost 200 km
od (our analysis time
ena. The associated
s⁻¹ to the NNW. In
n-velocity vector time
een constructed (see
nroughout. Maximum
approximately 56 km
was located near the
nences also show the
curred on 5 November
ity of approximately
ly. However, because
y appreciably (15–44
quences are generally
ne series is primarily

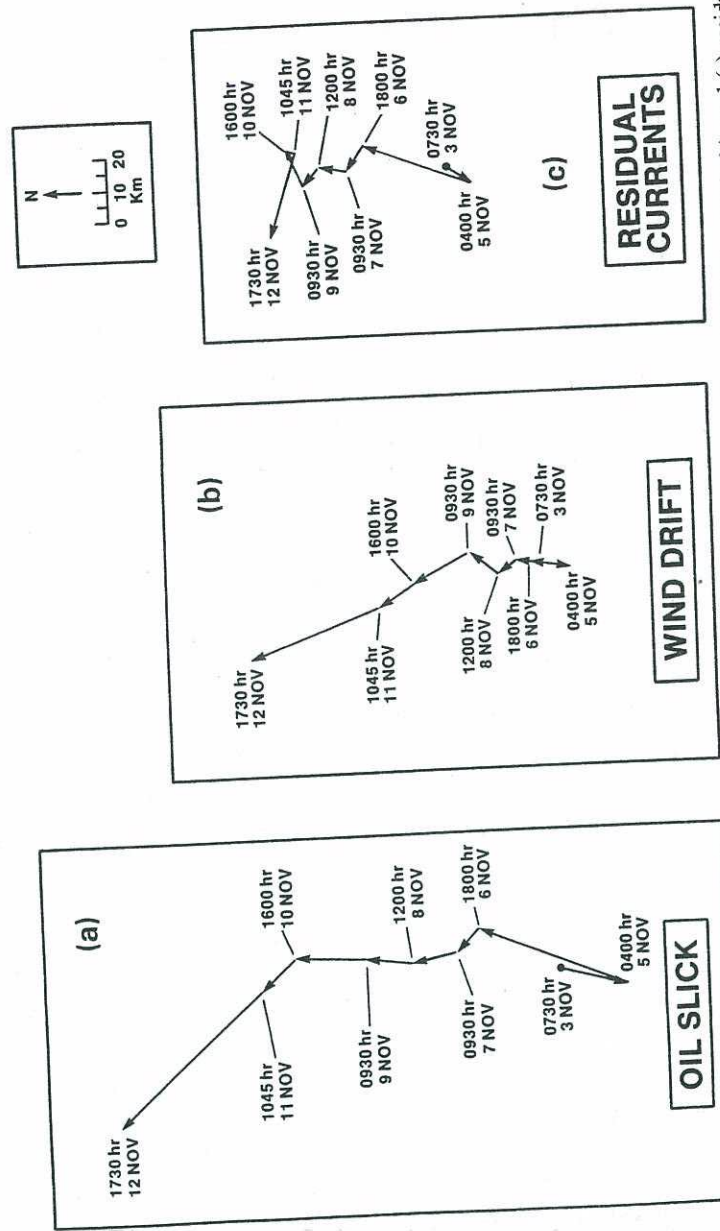

Fig. 8. Progressive vector diagrams of (a) oil-slick displacements, (b) wind-drift currents (based on NDBC buoy winds), and (c) residual currents.
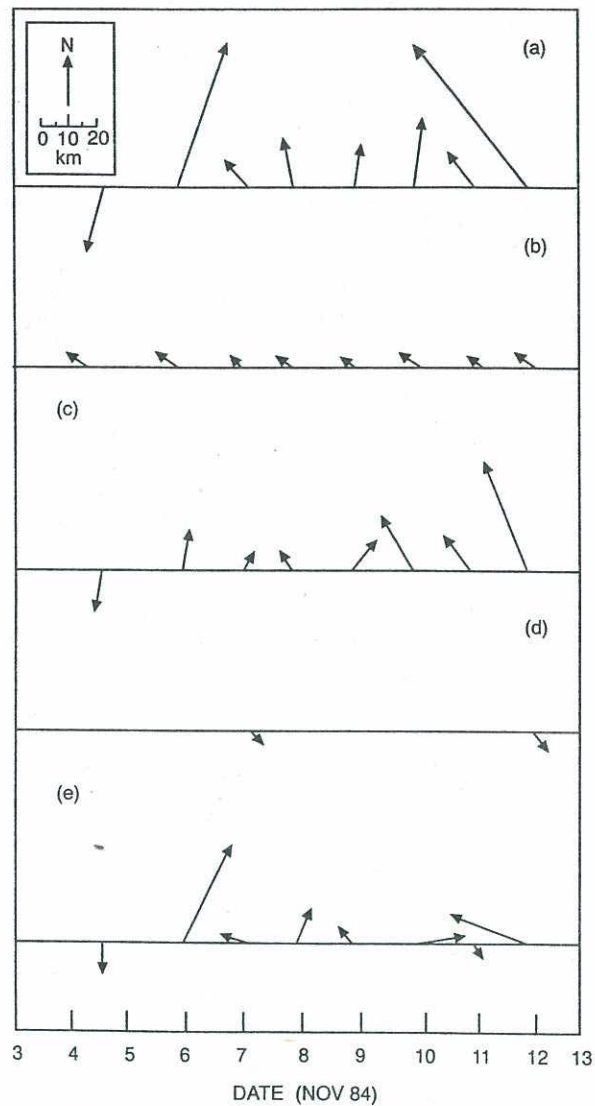
Fig. 9. Displacement-vector sequences for (a) oil spill, (b) permanent current, (c) wind drift, (d) tidal currents, and (e) residual currents.

Contributing processes†

To predict or hindcast the oil-slick drift or displacement associated with the *Puerto Rican* oil spill, large scale currents, surface-wind drift, and

† Processes that relate to oil-spreading and non-conservative effects with respect to the oil slick itself are not considered in these analyses.

Fig. 10. Lagra

tidal current
Such an app
such has bee
for the purp
the various
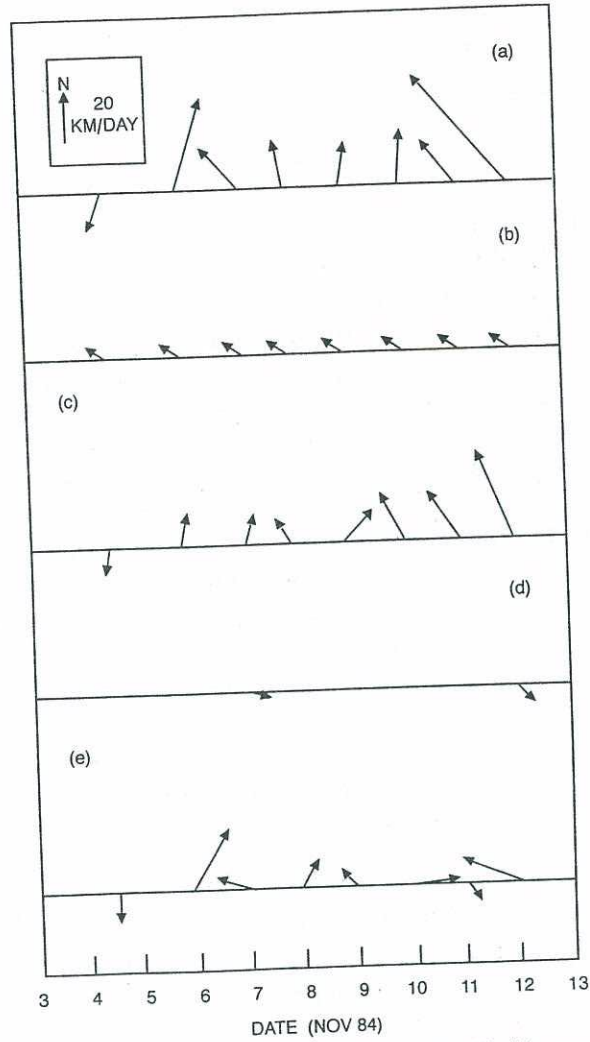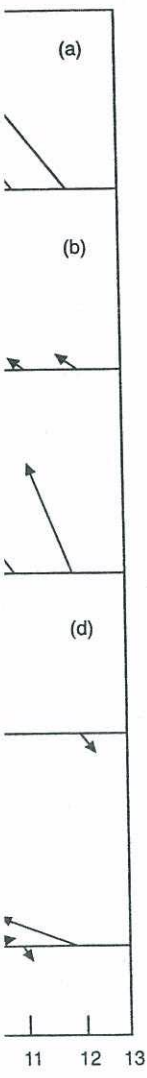vector addit
complex me
or impleme
large sampl

Fig. 10. Lagrangian velocity-vector sequences for (a) oil spill, (b) permanent current, (c) wind drift, (d) tidal currents, and (e) residual currents.

tidal currents were considered as likely generic sources of variability. Such an approach takes into account only advective processes and as such has been classified as an advective model (Murray, 1982). We assume for the purposes of our hindcast that the displacements associated with the various factors above can be combined by simple superposition (i.e. vector addition). We adopted this simplistic approach in lieu of more complex mechanistic models because such models are difficult to justify or implement in the absence of detailed dynamical data or relatively large samples (Jeffreys & Berger, 1992). We adopt the following formula-

tion to estimate the Lagrangian displacement of the oil spill with respect to a fixed point, which in our case is taken as the origin of the spill (i.e. its location on 3 November 1984 at 0730 GMT):

$$\mathbf{P}(t) = \int_0^t (\mathbf{V}_p(t) + \mathbf{V}_w(t) + \mathbf{V}_T(t)) \, dt \qquad (2)$$

We have explicitly included a large-scale current ($\mathbf{V}_p$), a wind-induced current ($\mathbf{V}_w$), and a tidal current ($\mathbf{V}_T$) in the above model. In our case, the large-scale current, $\mathbf{V}_p$, for example, may be dominated by seasonal or synoptic-scale flows. The parameter $\mathbf{V}_w$ represents that portion of the flow directly forced by local surface winds. This term includes the effects of waves and oil-to-water slippage (e.g. Smith, 1974), as well as the drift produced directly by the shear stress of the surface wind. The parameter $\mathbf{V}_T$ includes tidal effects that may be rotary in character offshore but tend to become more rectilinear closer to the coast. Because of the oscillatory nature of the tidal currents, their effects, averaged over a tidal cycle or more, are often small in comparison with the other components that make up the combined flow field. However, near the coastal boundary, this oscillatory perturbation in displacement can be a significant percentage of the encounter distance (i.e., the distance to landfall), so we have included this component in our analysis.

In this modeling approach, albeit greatly simplified, we assume that, if we subtract the model-derived displacements, $\mathbf{P}(t)$, from the observed oil-slick displacements, $\mathbf{OS}(t)$,

$$\mathbf{OS}(t) - \mathbf{P}(t) = \mathbf{R}(t) \qquad (3)$$

the resulting residuals, $\mathbf{R}(t)$, should contain no major deterministic components or statistical biases, given a high degree of model skill. Thus, we subsequently use $\mathbf{R}(t)$ as an indicator of our model's hindcasting performance. Note here that the residuals are linearly related to both the oil-slick displacements and the surface winds. We have also taken care to select the model parameters on an *a priori* basis. Thus, we use 'average values' from the historical literature and have resisted the tendency to 'tune' the model for the present problem. In the discussion, we indicate refinements that were suggested by the results of our analysis (i.e. *a posteriori*).

Large-scale flow regime

If large-scale 'permanent' or seasonal currents are significant, they must be taken into account in predicting oil-slick displacements. We searched the literature to find representative values for this model component.

: of the oil spill with respect
ıs the origin of the spill (i.e.
T):

$V_T(t))\, dt$ (2)

ırrent (V_p), a wind-induced
ove model. In our case, the
dominated by seasonal or
esents that portion of the
his term includes the effects
ı, 1974), as well as the drift
ırface wind. The parameter
character offshore but tend
:. Because of the oscillatory
raged over a tidal cycle or
he other components that
near the coastal boundary,
n be a significant percentage
: to landfall), so we have

nplified, we assume that, if
$P(t)$, from the observed oil-

(3)

n no major deterministic
legree of model skill. Thus,
f our model's hindcasting
linearly related to both the
We have also taken care to
sis. Thus, we use 'average
e resisted the tendency to
the discussion, we indicate
lts of our analysis (i.e. *a*

are significant, they must
isplacements. We searched
r this model component.

Monthly mean non-tidal currents were measured at the San Francisco Light Ship between 1915 and 1920 (Marmer, 1926) and indicate that there was a 'permanent' flow of order 5 cm s^{-1} to the NW year-around and that, for November, a speed of 6 cm s^{-1} and a direction of 300°T were representative.† Marmer pointed out that, since the prevailing winds were from the NW, the non-tidal flow could not be due to the local winds (although he apparently did not consider the possible influence of wind-stress curl). Surface-drifter observations reported by Conomos (1975) indicated that, for the Gulf of Farallones, a direction of 315°T was representative for the winter period. Current-meter measurements acquired during the Coastal Ocean Dynamics Experiment (CODE) program on the continental shelf between Bodega Bay and Pt Arena during the fall of 1981 indicated poleward flows of 5–7 cm s^{-1} approximately parallel to the coast at 9 m below the surface (Lentz & Chapman, 1989), values in close agreement with the surface values for speed and direction obtained by Marmer and Conomos. In addition, a poleward surface flow off San Francisco of about 6 cm s^{-1} is estimated from the dynamic topography shown in Fig. 2 for November (Wyllie, 1966). These independent determinations of the larger-scale flow near the coast are all generally consistent, even though they were formed over different time windows and by using different methods.

We have also performed a least-squares regression analysis by using the previous oil-slick velocities and the NDBC-buoy wind data, similar to that conducted by Winant *et al.* (1987), to estimate the forcing-response relationship between wind stress and near-surface along-shelf currents. With the same co-ordinate system as that used by Winant *et al.*, our results can be compared directly with theirs and indicate a significant relationship between the along-shore component of slick velocity and wind stress (Fig. 11). The *y* intercept is approximately 9 cm s^{-1} (compared with 11–13 cm s^{-1} found by Winant *et al.*), a value that reflects the along-shelf component of surface flow in the absence of wind forcing. Our slope is approximately 23 cm s^{-1}/dyn cm^{-2}, a value higher than that obtained by Winant *et al.* (14–16 cm s^{-1}/dyn cm^{-2}) and may reflect the oil-to-water slippage referred to in the previous section. Furthermore, our results are based on Lagrangian-flow estimates with many fewer degrees of freedom than the Winant *et al.* value (based on Eulerian measurements), plus the fact that there is only one value at the high end of the along-shore-

† Annual and monthly-averaged currents were recently measured off the central California coast (38·6°N, 123·5°W and 37·4°N, 122·9°W) during the superCODE program (Strub *et al.*, 1987). However, the shallowest level at which these data were acquired was 35 m, a depth that may have been too deep to be representative of the circulation occurring in the upper wind-driven surface layer.
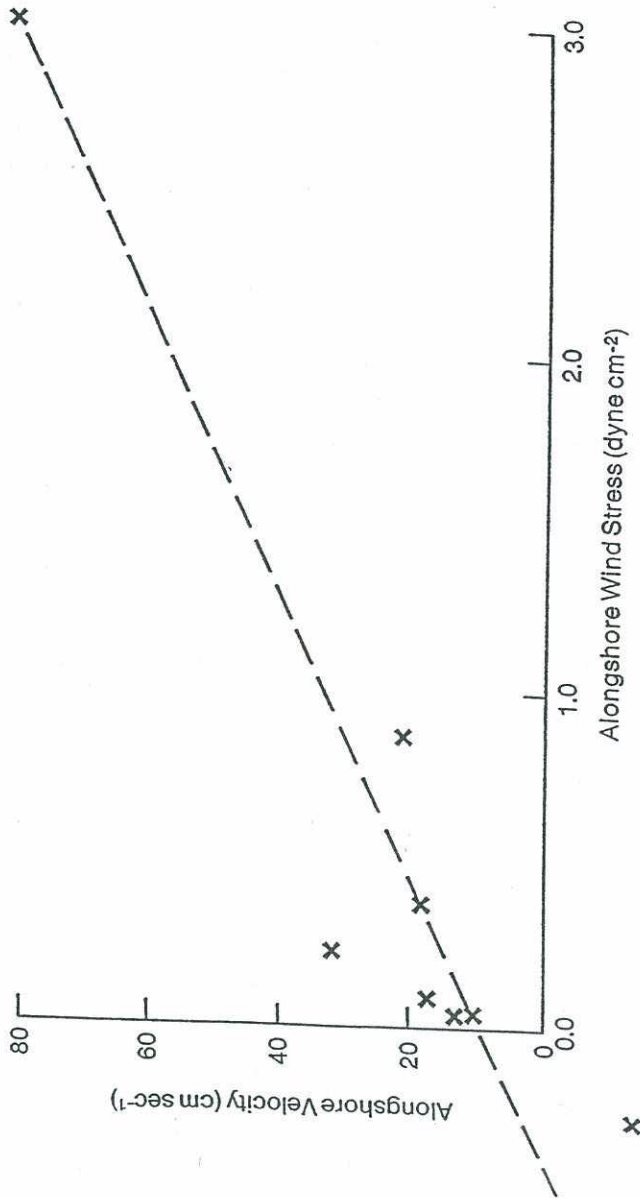
Laurence C. Breaker, Alan Bratkovich

velocity/wind-stress rel
consistent with prior f
of this type utilizing :
of approximately 9 c
(1926), Lentz & Chap
for the large-scale flo
large-scale current of
entire oil-spill trajecto

Surface winds

A number of studies h
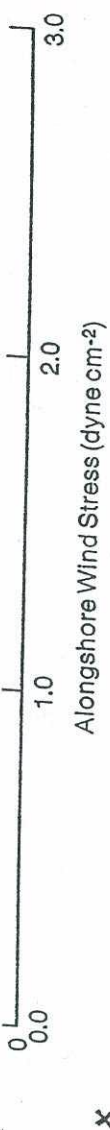in accordance with tl
local wind forcing. H
Tomczak (1964) cond
at about 4·3% of its
escaped from the *Tc*
movement associated
assuming that the oi
about 3·4% of its sp
by Schwartzberg (19
wind factor of 3·5%
Mattson (1977) and
basis of the *Argo M*
appropriate value fo:

The wind-induced
factor in oil-spill-tr
surface-wind shear s'
oil-to-water differen'
the wind-factor for:
various physical pro
because this approa(
various oil-spill stuc
the studies cited abc

where **W** represents
is taken to be the s:
of earth rotation is
than approximately

To account for tl
with the *Puerto R*

Fig. 11. Regression of along-shelf (along-shelf co-ordinate equals 317°T) oil-slick velocities versus along-shelf component of wind stress, based on Fig. 9a and 9c (or Fig. 10a and 10c). The y intercept is approximately 9 cm s^{-1}, and the slope is approximately 23 cm s^{-1}/dyn cm^{-2}.

velocity/wind-stress relationship in our case. Nevertheless, these results are consistent with prior findings in this area and represent the first analysis of this type utilizing actual oil-slick-trajectory data. The intercept value of approximately 9 cm s^{-1} is close to the values obtained by Marmer (1926), Lentz & Chapman (1989), and the dynamic topography in Fig. 2, for the large-scale flow. Thus we include a conservative estimate for the large-scale current of 6 cm s^{-1} at 315°T in our model, applicable to the entire oil-spill trajectory.

Surface winds

A number of studies have shown that oil on the surface of the ocean moves in accordance with the prevailing 'drift' currents, usually in response to local wind forcing. From observations of oil spilled in the North Sea, Tomczak (1964) concluded that the oil in this case moved with the wind at about 4·3% of its speed. On the basis of observations of the oil that escaped from the *Torrey Canyon*, Smith (1968) concluded that the oil movement associated with that spill could be accurately simulated by assuming that the oil moved in the same direction as the wind but with about 3·4% of its speed. A wind factor of 3·66% ± 0·17% was obtained by Schwartzberg (1970) for quiet open water. Hoult (1972) indicated a wind factor of 3·5% in oil-spill-trajectory forecasting. Finally, Gross & Mattson (1977) and Lissauer & Welsh (1978) also concluded, on the basis of the *Argo Merchant* oil spill, that a value of 3·5% represents an appropriate value for the surface-wind drift factor.

The wind-induced current, when parameterized in the form of a wind factor in oil-spill-trajectory models, includes not only the effect of surface-wind shear stress but also the effects of surface gravity waves and oil-to-water differential velocities (i.e. oil-to-water slippage). As a result, the wind-factor formulation does not explicitly take into account the various physical processes that contribute to surface-wind drift. However, because this approach is straightforward and has been so widely used in various oil-spill studies, we have adopted it here. Thus, on the basis of the studies cited above, we express the wind-induced surface drift as:

$$\mathbf{V}_w = 0.035\mathbf{W} \tag{4}$$

where $\mathbf{W}$ represents the mean local wind velocity and the direction of $\mathbf{V}_w$ is taken to be the same as that of $\mathbf{W}$. In some oil-spill models, the effect of earth rotation is included but is always assumed to be small (i.e. less than approximately 20°).

To account for the effect of the wind on the oil movement associated with the *Puerto Rican* spill, surface-wind data acquired from NDBC

Fig. 11. Regression of along-shelf (along-shelf co-ordinate equals 317°T) oil-slick velocities versus along-shelf component of wind stress, based on Fig. 9a and 9c (or Fig. 10a and 10c). The y intercept is approximately 9 cm s^{-1}, and the slope is approximately 23 cm s^{-1}/dyn cm^{-2}.

Alongshore Wind Stress (dyne cm^{-2})

buoys in close proximity to the oil slick are used to estimate surface-drift velocities by using the above wind-drift relationship. This combination of PVD displacement vectors consists of the first two vectors taken from NDBC buoy 46012 (37·4·N, 122·7°W), vectors 3 and 4 taken from buoy 46026 (37·8°N, 123·2°W), vectors 5, 6 and 7 taken from buoy 46013 (39·2°N, 124·0°W), and the last vector taken from buoy 46014 (40·8°N, 124·5°W). Based on these winds, a composite of PVD, displacement, and velocity-vector time series for the wind-drift currents was constructed (Figs 8b, 9c and 10c).

In a similar manner to the oil-slick PVD, the composite wind-drift PVD indicates southward motion between 3 and 5 November. Over-all, drift-current displacements indicate net motion to the north and NNW, respectively. Unlike the oil-slick PVD, however, the northernmost vector from the drift-current PVD (buoy 46014) indicates motion that is approximately northward (as compared with NW) from 10 to 12 November. This discrepancy is due, at least in part, to the 'steering' influence of the shelf bathymetry experienced by the oil as it approached Pt Reyes and the coastal region between Pt Reyes and Pt Arena. In general, the wind-drift displacements are similar to, but smaller than, the displacements obtained from the oil-slick trajectory *per se*. In particular, the displacement-vector sequences show that, although the wind reversed direction on or about 5 November, the magnitude of the corresponding wind-drift displacement is significantly smaller (approximately 54 km compared with 14 km) than the observed oil-slick displacement at this time. Thus it is unlikely that this abrupt change in oil-slick displacement can be explained by local wind forcing alone.

Tidal currents

Tidal currents enhanced or retarded the oil in its over-all northward displacement depending on the exact phase, amplitude, and direction of the local tides. The tides in the Gulf of the Farallones are mixed but mainly semidiurnal. Offshore, the tidal currents in the Gulf and further north are rotary; closer to the coast they become rectilinear (Fig. 12). Tidal currents near the entrance of San Francisco Bay (i.e. the Golden Gate) are anomalously intense and reach speeds of over 200 cm s^{-1} at maximum ebb (US Dept, of Commerce, 1973).

Because the tidal flows were not known precisely at the various locations where the oil-spill sightings were made, we estimate tidal effects along the oil-spill trajectory by extrapolating tidal-current data acquired at nearby locations, as given by Marmer (1926), the NOS Tidal Current Tables (1984*a*), and Rosenfeld & Beardsley (1987). Figure 12 shows tidal-
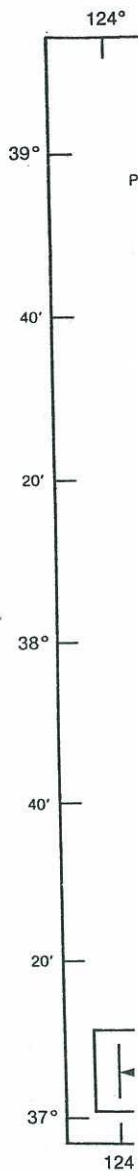
Fig. 12. L
Arena. Offs

d to estimate surface-drift
ship. This combination of
two vectors taken from
3 and 4 taken from buoy
taken from buoy 46013
om buoy 46014 (40·8°N,
PVD, displacement, and
currents was constructed

the composite wind-drift
d 5 November. Over-all,
to the north and NNW,
the northernmost vector
ndicates motion that is
from 10 to 12 November.
'steering' influence of the
pproached Pt Reyes and
na. In general, the wind-
than, the displacements
rticular, the displacement-
d reversed direction on
corresponding wind-drift
nately 54 km compared
ement at this time. Thus
ick displacement can be

n its over-all northward
plitude, and direction of
arallones are mixed but
in the Gulf and further
me rectilinear (Fig. 12).
sco Bay (i.e. the Golden
ls of over 200 cm s⁻¹ at

isely at the various loca-
we estimate tidal effects
al-current data acquired
, the NOS Tidal Current
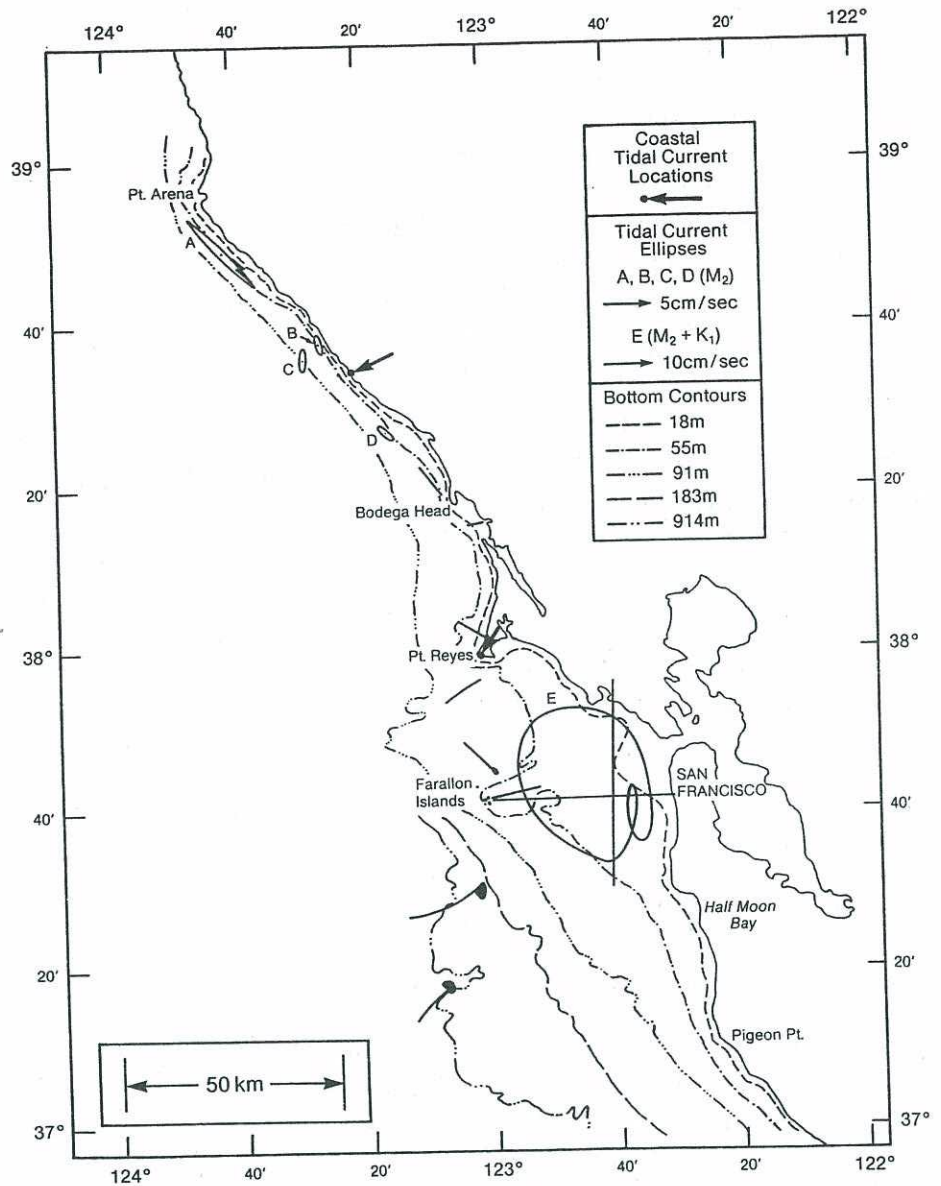). Figure 12 shows tidal-

Fig. 12. Locations of tidal-current data in the Gulf of the Farallones and north to Pont Arena. Offshore locations are indicated by tidal ellipses and locations on the coast are indicated by arrows.

current ellipses at several locations within the general area of the oil spill. The tidal-current ellipse off San Francisco (Marmer, 1926) undoubtedly contains at least some influence from the strong tidal currents in and around the Golden Gate. Current ellipses farther north along the coast (Rosenfeld & Beardsley, 1987) indicate generally weaker tidal flows. Tidal currents at two coastal locations are also included, one at Pt Reyes and a second at a point midway between Bodega Head and Pt Arena. These sources of tidal-current information have been used to estimate the tidal currents at the mid-points between oil-spill sightings by taking into account the changes in current velocity due to increases (or decreases) in bottom depth. These adjustments were made by assuming that the rate of energy transmission is conserved as the tide moves into shallower water. The estimated ellipses were digitized every hour to obtain the u and v velocity components, which were then averaged over the period between successive oil-spill sightings.† No allowances have been made for the inherent variability associated with tidal currents or for possible errors in their measurement.

The mean tidal currents at each mid-point location are shown in Fig. 10(d). Owing to the generally low velocities and the oscillatory nature of the tidal currents, their cumulative effects are relatively small; however, between oil-slick sightings 3 and 4 and between sightings 8 and 9, they are non-negligible. Higher tidal-current velocities between locations 8 and 9 are based on the results of Rosenfeld & Beardsley, who found that tidal currents along the coast increase significantly between about 38·5°N and 39°N.

Residual analysis

Since we have constructed our model on the basis of parameterizations and values from the literature, residuals could be weakly (or strongly) correlated with the original series depending on the relative effectiveness of the model. In the limit, a 'perfect' model would be expected to produce residuals that have only an insignificant correlation and a relatively small variance compared with the original series. In accordance with eqn (3) and our previous discussion, we subtract the sum of the large-scale, wind-drift, and tidal-current displacements from the original oil-slick

---

† Clarke and Battisti (1981) present a model which uses coastal sea-level measurements to calculate a complex along-shore wavenumber, which in turn is used to predict along-shore tidal currents. However Rosenfeld & Beardsley (1987) found that this model was unable to predict correctly the variability of the along-shore tidal current in the coastal region between Pt Reyes and Pt Arena, and thus it has not been used in this study to estimate tidal currents.

---

displacements to prod
These residuals are sho
all displacements assoc
(approximately 50 km
compared with the oi
indicates a residual flo
for the oil slick itsel
contains individual v
with either the large-sc
drift displacements ge

A sensitivity analys
wind factor actually
sense), our own obse
duced the smallest re
approximately 5%), a
reported elsewhere
(0·8–5·8%). However,
of 3·5% for several re
fact that it minimize
somewhat arbitrary,
wind affect the magn
was obtained from a
of 3·5% was estimate
sample sizes far excee

Vector correlations

To determine the deg
the various modeled
Details concerning th
their significance lev
The correlation coeff
vector sequences are

Results obtained
approximately 0·51
true correlation is nc
of eight.† According
oil slick and the wir

---

† These results assume t
tainly violated in this st
subsampling usually ach
case was too small (i.e. e

ovich

neral area of the oil spill.
rmer, 1926) undoubtedly
ng tidal currents in and
er north along the coast
ally weaker tidal flows.
included, one at Pt Reyes
ega Head and Pt Arena.
been used to estimate the
l sightings by taking into
ncreases (or decreases) in
assuming that the rate of
ves into shallower water.
r to obtain the u and v
over the period between
have been made for the
s or for possible errors in

cation are shown in Fig.
the oscillatory nature of
elatively small; however,
sightings 8 and 9, they
ties between locations 8
eardsley, who found that
ly between about 38·5°N

sis of parameterizations
be weakly (or strongly)
e relative effectiveness of
be expected to produce
on and a relatively small
accordance with eqn (3)
sum of the large-scale,
m the original oil-slick

oastal sea-level measurements
turn is used to predict along-
7) found that this model was
re tidal current in the coastal
been used in this study to esti-

displacements to produce a sequence of residual-displacement vectors. These residuals are shown in Figs 8(c), 9(e) (and 10(e)). Although the overall displacements associated with the residual currents are relatively small (approximately 50 km to the north and approximately 20 km to the west) compared with the oil-slick PVD, they form an organized pattern that indicates a residual flow to the WNW, similar to the displacement pattern for the oil slick itself. The residual-displacement sequence (Fig. 9(e)) contains individual vectors whose magnitudes exceed those associated with either the large-scale or the tidal-current components. Only the wind-drift displacements generally exceed those associated with the residuals.

A sensitivity analysis was conducted to determine what value for the wind factor actually yielded the smallest residuals (in the mean-square sense), our own observations being used. A wind factor of 4·4% produced the smallest residuals (and reduced the mean-square residuals by approximately 5%), a wind factor well within the range of wind factors reported elsewhere and summarized by Stolzenbach *et al.* (1977) (0·8–5·8%). However, as indicated before, we chose to use a wind factor of 3·5% for several reasons. First, to use a wind factor based only on the fact that it minimizes the residuals for this one limited case appears somewhat arbitrary, since a number of other factors in addition to the wind affect the magnitude of the residuals. Second, our 'optimal' value was obtained from an extremely small sample (eight), whereas the value of 3·5% was estimated from a number of independent studies where the sample sizes far exceeded our own.

Vector correlations

To determine the degree of similarity between the oil-slick movement and the various modeled drift components, vector correlations were calculated. Details concerning the method of calculating these vector correlations and their significance levels are contained in the work of Crosby *et al.* (1993). The correlation coefficients for the various combinations of displacement-vector sequences are given in Table 2.

Results obtained by Crosby *et al.* indicate that vector correlations of approximately 0·51 or greater are statistically significant (i.e. that the true correlation is non-zero) at the 95% confidence level for a sample size of eight.† According to Table 2, only the vector correlations between the oil slick and the wind drift, and between the oil slick and the residuals,

† These results assume that the observations are independent, an assumption almost certainly violated in this study. In cases where the sample sizes are sufficient, appropriate subsampling usually achieves the desired independence. However, the sample size in this case was too small (i.e. eight) to allow subsampling.

TABLE 2
Vector Correlations between the Oil Slick, the Various Current Components and the Residual Current Displacements[a]

	Displacement vector correlations				
	Oil-slick	Large-scale current	Wind drift	Tidal current	Residuals
Oil-slick	—	0·34	0·55	0·50	0·63
Large-scale current	—	—	0·39	0·36	0·34
Wind drift	—	—	—	0·40	0·40
Tidal current	—	—	—	—	0·46
Residuals	—	—	—	—	—

[a] Sample size = 8 in each case.

may be statistically significant. However, because of the small sample size involved and the likelihood of serial correlation in the observations, the significance of these vector correlations should be interpreted with caution.

The relatively high correlation between the wind-drift and the oil-slick displacement vectors suggests the importance of the local winds in contributing to the displacement of the oil. The high correlation between the oil slick and the residuals suggests that factors in addition to local wind-driven effects influenced the original oil-slick displacement or that some of the original 'signal' still remains in the residual field and was not accurately modeled or extracted. Alternatively, it is possible (but unlikely) that the model was 'perfect', but errors in the input data led to inaccuracies in the trajectory simulation. We subsequently consider the possibility that the primary residual observed on 5 November was related to an unresolved large-scale feature in the flow field.

DISCUSSION

During the fall, the Davidson Current develops along the California coast north of Pt Conception (approximately 35°N; Fig. 2). This surface countercurrent flows inshore of the equatorward-flowing California Current extending about 100 km offshore and is strongest between November and January (Hickey, 1979). The coastal winds along central and Northern California were generally from the north (i.e. upwelling-favorable) prior to the ACR in the Gulf of the Farallones. Between the last week in October and the first week in November, these winds had become predominantly from

the south (i.e.
(Strub & Jam
Current. SSTs
gradually incre
baroclinic char
of the Davids

With respec
forecasts were
the oil spill e
forecasting dif
together with
1984).

According
often accomp
the onset of
have expecte
associated wi
flow regime.
and surface-
during this p

SSTs show
waters, possi
account for t
period of the
we compare
13 (approxin
temperature
oceanic surf
(v) of 20 kr
SST ($\partial T/\partial t$)
1984b) and (
obtained di
coast indica
observation
that values (
The close ag
rates of cha
Farallones,
November
Although t
change dur
central Cal

Current Components and the
^{a}

	correlations	
	Tidal current	Residuals
	0·50	0·63
	0·36	0·34
	0·40	0·40
	—	0·46
	—	—

of the small sample size
on in the observations,
uld be interpreted with

d-drift and the oil-slick
of the local winds in
igh correlation between
ors in addition to local
k displacement or that
sidual field and was not
s possible (but unlikely)
data led to inaccuracies
sider the possibility that
related to an unresolved

along the California
N; Fig. 2). This surface
wing California Current
est between November
ig central and Northern
lling-favorable) prior to
ast week in October and
he predominantly from

the south (i.e. downwelling-favorable), consistent with the fall transition (Strub & James, 1988) and the seasonal development of the Davidson Current. SSTs along central California (between 37·4°N and 39·2°N) gradually increased during this period, this being indicative of a seasonal baroclinic change in the upper ocean, also consistent with the development of the Davidson Current.

With respect to the ACR in the Gulf of the Farallones, oil-spill-trajectory forecasts were unable to predict accurately the sudden major change that the oil spill experienced on 5 November (Herz & Kopec, 1985). These forecasting difficulties were attributed to the onset of the Davidson Current together with a complex eddy pattern in the San Francisco Bight (Galt, 1984).

According to Hickey (1979), the onset of the Davidson Current is often accompanied by significant changes in water properties. Thus, if the onset of the Davidson Current did occur on 5 November, we might have expected to observe changes in the local SST and salinity fields associated with the temperature/salinity properties that characterize this flow regime. To address this point, we have examined the available SST and surface-salinity data that were acquired at the Farallon Islands during this period (SIO, 1985).

SSTs shown in Fig. 13 suggest that poleward advection of warmer waters, possibly associated with the onset of the Davidson Current, could account for the systematic increase in temperature that occurred during the period of the ACR in the Gulf of the Farallones. To test this hypothesis, we compare the observed local rate of change in SST ($\partial T/\partial t$) from Fig. 13 (approximately 0·12°C/day) with an estimate of the local change in temperature associated with the net poleward advection of heat in the oceanic surface layer ($v \cdot \partial T/\partial y$). We use an average along-shore velocity (v) of 20 km day^{-1} (Fig. 10) and an along-shore spatial derivative for SST ($\partial T/\partial t$) for November of 0·55°C/100 km (US Dept of Commerce, 1984b) and obtain a value for $v \cdot \partial T/\partial y$ of 0·11°C/day. Coastal SST gradients obtained directly from the NDBC buoys along the central California coast indicated slightly higher values, but, because they represent point observations relatively near the coast (approximately 20 km), it was felt that values obtained from spatially averaged fields were more representative. The close agreement between the observed local and the estimated advective rates of change in SST during the period of the oil spill in the Gulf of the Farallones, has allowed us to consider the possibility that the ACR on 5 November was in fact, related to the onset of the Davidson Current. Although the surface salinities shown in Fig. 13 indicate essentially no change during the period of interest, we note that conditions along the central California coast may have been more homogeneous with respect
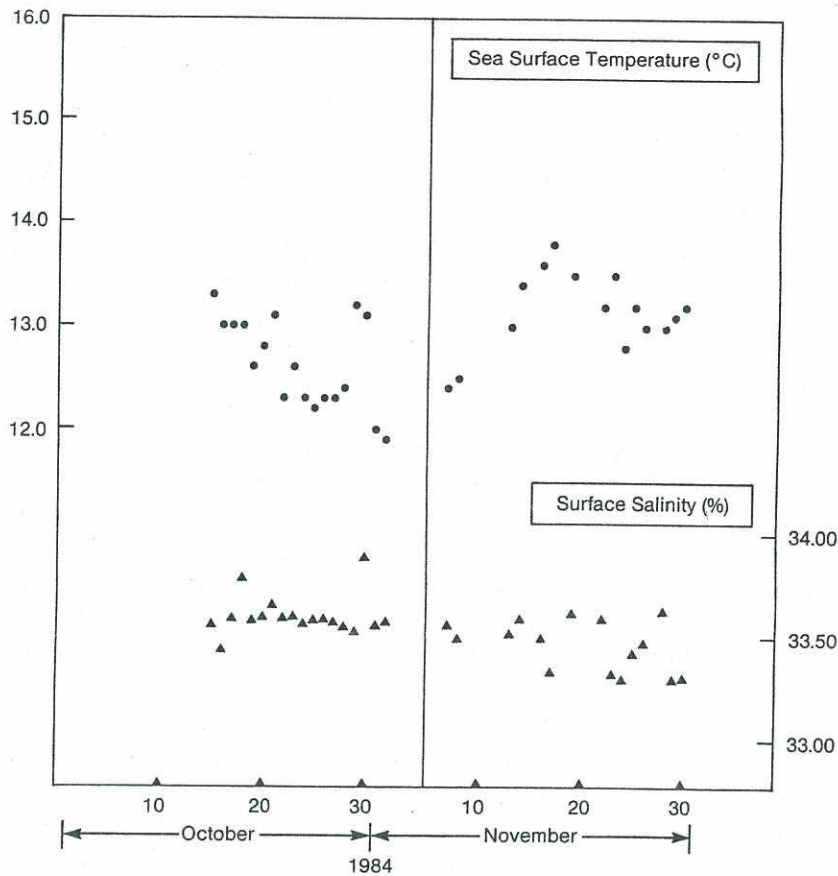
Fig. 13. Daily observations of sea-surface temperature and sea surface salinity acquired at the Farallon Islands from 15 October to 30 November 1984.

to this property (the along-coast climatological gradient in surface salinity for this region and period is only approximately 0·07 ppt/100 km (Churgin & Halminski, 1974)). Finally, on the basis of the eighteen temperature profiles acquired in or near the Gulf of the Farallones between 15 October and 19 November (Fig. 7), the one profile acquired after 5 November (i.e. 19 November) has the highest temperatures below about 55 m, consistent, at least at depth, with the arrival of warmer waters from the south.

Another indication of conditions consistent with the development of the Davidson Current is the so-called fall transition (Strub & James, 1988). According to Strub & James, the fall transition signals the onset of the fall/winter downwelling regime off the US West Coast. The fall transition coincides with the onset of seasonal storm activity and is accompanied by (sustained) increases in both northward wind stress and coastal sea level. Based on sea-level data over nine years, the fall transition

ace Temperature (°C)

Surface Salinity (%)

34.00

33.50

33.00

20   30

)er ⟶

.nd sea surface salinity acquired
) November 1984.

gradient in surface salinity
0·07 ppt/100 km (Churgin
the eighteen temperature
llones between 15 October
red after 5 November (i.e.
w about 55 m, consistent,
ters from the south.

with the development of
ansition (Strub & James,
ansition signals the onset
US West Coast. The fall
al storm activity and is
orthward wind stress and
ie years, the fall transition

typically occurs around 1 November. Thus, the wind-stress data in Fig. 4 and the date of the ACR in the Gulf of the Farallones (5 November 1984) are both consistent with the occurrence of the fall transition and thus the oceanic conditions that are necessary for and consistent with the development of the Davidson Current. The dynamical details of the transition process have yet to be resolved. The suggestion of a very slight increase in mean sea level (see Fig. 6) of the order of 5–10 cm occurs from Monterey northward, after the 5 November episode and could reflect the onset of a sustained larger-scale flow to the north.

In summary, conditions were favorable for the development of the Davidson Current during the period of the *Puerto Rican* oil spill. These conditions, taken together with the close agreement in the observed local rate of change in SST, and the estimated advective-flux contributions to changes in SST, are generally consistent with the onset of the Davidson Current in the Gulf of the Farallones.

From the previous hindcast analysis, it is not possible to determine whether or not deficiencies in our model were due to inadequate model formulation or to inaccuracies in the input data, or both. By inadequate model formulation, we recognized the possibility that either (i) not all of the important flow components were included, or (ii) those components that were included were not adequately parameterized. For example, the use of a wind factor to account for wind drift grossly oversimplifies the problem. According to Stolzenbach et al. (1977), wave-induced transport is expected to contribute significantly to wind drift, and additionally the wave-induced and the wind-induced transports may best be parameterized separately. Such a partitioning is further supported by the theoretical results of Huang (1979), where surface-drift currents are generated by both direct wind stress, based on Ekman dynamics, and Stokes' drift, derived from the surface-wave motion. Additionally, Reisberg et al. (1973) indicate that, at lower wind speeds, wave-induced transport due to Stokes' drift augments the wind drift, whereas, at higher wind speeds, the waves cause a net decrease in drift velocity. Relative oil-to-water motion or slippage also influences the wind factor. According to Smith (1974), oil-to-water slippage may account for up to 50% of the wind drift experienced by the oil.

The simple, *a priori* model used in this study would have exhibited improved performance if the correlation between the oil-spill trajectory and the residuals (produced after the flow components taken into account by the model had been removed) had been relatively low (i.e. not statistically significant). This was not the case. The largest part of the covariability between the oil-slick trajectory and the residuals was undoubtedly due to the major change in oil-spill movement that occurred on 5 November and whose influence clearly remains in the residual field (e.g. Fig. 9(e)).

This strong residual signal cannot be explained by the winds alone, since the magnitude of this sudden reversal exceeded that predicted by the change in winds *per se* by almost 400% (see Figs 9(a) and 9(c): ~54 km as compared with ~14 km). Even when the wind factor was varied to minimize the residuals, the 'optimum' wind factor so obtained (4·4%) reduced the mean square residuals by only about 5%. After this reversal took place, we noted that the local wind-drift displacements were similar to, but generally less than, those experienced by the oil slick itself.

It is likely that inaccuracies or unrepresentativeness of the input data affected model performance. For example, wind-stress curl, which is important along the central California coast (Nelson, 1977) was not taken into account as a large-scale forcing function. Furthermore, uncertainties exist in locating the exact centroid of the oil slick itself at the various locations where sightings were taken. For example, we have assumed that the surface manifestation of the slick remained intact throughout the study period. Finally, our lack of knowledge concerning the exact value of, or parameterization for, the wind factor leads to significant uncertainties in estimating the wind drift. We note, however, that such arguments almost certainly will not explain the large residual displacement that occurred on 5 November 1984.

With the exception of the ACR on 5 November, wind drift alone accounts for a significant fraction of the oil-spill displacement during its passage through the Gulf of the Farallones and further north, uncertainties in the wind factor notwithstanding. The importance of the local winds in determining the trajectory of the oil was indicated by the high correlation between the oil-spill displacements and the corresponding wind-drift displacements. Over-all, wind drift accounted for approximately 62% of the total displacement experienced by the oil over its trajectory, and, in six out of eight cases, the wind direction was within ±25° of the direction of the oil-slick displacement. The importance of wind drift during this oil spill is consistent with the results from a number of other oil-spill studies where local wind effects were also found to be important (e.g. the *Gerd Maersk* oil spill (Tomczak, 1964); the *Torrey Canyon* oil spill (Smith, 1968); the *Argo Merchant* oil spill (Pollack & Stolzenbach, 1978)).

With respect to the ACR in the Gulf of the Farallones, the observations presented here do not, in all cases, clearly demonstrate that this reversal was, in fact, related to the onset of the Davidson Current. For example, examination of the sea-level time series (Fig. 6) indicates a surge-like increase in sea level off central California both at Monterey (25–30 cm) and San Francisco (15 cm) that coincided with the ACR in the Gulf of the Farallones. However, this increase was only weakly sustained at best, contrary to our expectations if a major seasonal flow regime such

by the winds alone, since
d that predicted by the
s 9(a) and 9(c): ~54 km
d factor was varied to
tor so obtained (4·4%)
t 5%. After this reversal
splacements were similar
he oil slick itself.

veness of the input data
d-stress curl, which is
son, 1977) was not taken
rthermore, uncertainties
ck itself at the various
nple, we have assumed
ed intact throughout the
rning the exact value of,
significant uncertainties
r, that such arguments
dual displacement that

mber, wind drift alone
displacement during its
rther north, uncertainties
ce of the local winds in
by the high correlation
orresponding wind-drift
approximately 62% of
r its trajectory, and, in
in ±25° of the direction
vind drift during this oil
of other oil-spill studies
nportant (e.g. the *Gerd*
Canyon oil spill (Smith,
zenbach, 1978)).

arallones, the observa-
demonstrate that this
Davidson Current. For
es (Fig. 6) indicates a
rnia both at Monterey
led with the ACR in the
s only weakly sustained
asonal flow regime such

as the Davidson Current had become permanently established at this time. Additionally, Figs 9 and 10 indicate that most of the poleward flow following the ACR on 5 November can be accounted for by the wind alone. A stronger non-wind-driven (i.e. permanent) component might be expected to accompany the development of a seasonal flow regime such as the Davidson Current. Moreover, the Davidson Current in early November 1984 was apparently advancing northward along the central California coast just prior to its arrival off San Francisco (Galt, 1984). Poleward development of the Davidson Current is contradictory, however, to descriptions given by Schwartzlose (1963) and Nelson (1976) for seasonal current development off the US West Coast. According to drift-bottle results from Schwartzlose (1955–60), the Davidson Current first develops along Washington and Oregon in August or September, and then by October it may appear as far south as Point Conception, indicating that the development of the Davidson Current advances equatorward, not poleward, along the California coast. Monthly charts of ship drift off the US West Coast (Nelson, 1976) also indicate that poleward flow begins first off Vancouver Island and then progresses southward. These apparent inconsistencies in the phasing of the seasonal development of the Davidson Current underscore our over-all lack of knowledge concerning the seasonal development (and cessation) of the various flows that make up the California Current System.

Although the onset of the Davidson Current provides one explanation for the ACR in the Gulf of the Farallones, other explanations are possible. For example, the upwelling relaxation phenomenon analyzed and modeled by Send *et al.* (1987) may have contributed to the surge-like behaviour that occurred on 5 November, particularly near the coast. The Send *et al.* (1987) 'surge' heat-transport mechanism is a response to the cessation of upwelling-favorable winds during spring and summer along the coast of Northern California. The along shelf current response reverses from equatorward (approximately -20 cm s^{-1}) to poleward (approximately $+20$ cm s^{-1}). The cross-shelf response is much weaker. The offshore scale of the warm, coastally trapped surge is 10–25 km, and its duration is in the range of 4–12 days. Thus, the cross-shelf spatial scale for this type of surge event may be too small (by a factor of two or so) to be consistent with the ACR in the Gulf of the Farallones. Additionally, the event reported here occurred in the fall rather than in the spring or summer; thus, the seasonal wind forcing and phase of the annual heating–cooling cycle could differ significantly from the conditions under which the Send *et al.* mechanism was obtained.

Coastal trapped waves provide another possible explanation for the ACR in the Gulf of the Farallones. These coastally trapped long waves

are often produced by synoptic atmospheric disturbances far removed from the area of interest. These waves propagate poleward along the west coast of the USA and transmit 'information' on events that have occurred previously at equatorward locations. Chapman (1987) applied a coastal-trapped-wave model to the coast of Northern California during the CODE program. Specific application of Chapman's results to the Gulf of the Farallones is complicated by the very irregular coastal morphology and bathymetry in this area. However, his results do indicate that the along-shelf modal-velocity structure extends offshore to the continental-shelf break and the upper slope, with the maximum current response occurring along the inner shelf. The expected amplitude of the along-shelf current response is 10–20 cm s^{-1}. The wave-mode-phase speeds and periods are at least about 100 km day^{-1} and 3–10 days, respectively. Since the wave parameters of Chapman's model are sensitive to both bathymetry and stratification, it is difficult to apply his results directly to the ACR in the Gulf of the Farallones. The offshore scale of the coastal-trapped-wave response and the amplitude of the along-shelf current response are both consistent with the observed ACR event. However, other factors argue against using a coastal-trapped-wave event to explain the ACR; these include (i) the local sea-level response exceeded that expected for coastal trapped waves by roughly a factor of two (approximately 20 cm compared with about 10 cm) given the amplitude of the current response; (ii) there was no clear signal in sea level south of Monterey that would have been expected for waves generated further south along the west coast; and (iii), the increase in sea level at Monterey, San Francisco, and Crescent City occurred more or less simultaneously, contrary to the arrival pattern (i.e. delays) that would be expected for a propagating wave with a phase speed of approximately 100 km day^{-1}. However, we do not completely rule out the possibility of a coastal-trapped-wave event for several reasons: first, there are inherent difficulties in deciphering sea-level records; second, it is possible that the coastal-trapped-wave generation process could have occurred locally (i.e. in the Gulf of Farallones itself) rather than at some remote location further south along the west coast, and finally, a somewhat similar situation occurred off the coast of Oregon in 1973, where coastal trapped waves were held responsible for a major current reversal occurring over a two-day period in that year (Kundu *et al.*, 1975).

The results from the CODE Program off Northern California have revealed a rich variety of circulation features in this region that include coastal jets, eddies, squirts, fronts, and filaments. Thus it is also possible that the ACR in the Gulf of the Farallones could have resulted from a transient encounter with one of these features. The availability of

disturbances far removed
agate poleward along the
tion' on events that have
Chapman (1987) applied a
thern California during the
nan's results to the Gulf of
gular coastal morphology
sults do indicate that the
ffshore to the continental-
aximum current response
l amplitude of the along-
ve-mode-phase speeds and
l 3–10 days, respectively.
odel are sensitive to both
pply his results directly to
shore scale of the coastal-
f the along-shelf current
ACR event. However, other
wave event to explain the
se exceeded that expected
two (approximately 20 cm
le of the current response;
n of Monterey that would
er south along the west
terey, San Francisco, and
neously, contrary to the
pected for a propagating
0 km day^{-1}. However, we
oastal-trapped-wave event
difficulties in deciphering
the coastal-trapped-wave
e. in the Gulf of Farallones
ther south along the west
occurred off the coast of
were held responsible for
-day period in that year

Northern California have
n this region that include
s. Thus it is also possible
could have resulted from
ures. The availability of

AVHRR satellite data would have been extremely helpful in identifying possible circulation anomalies that could have contributed to the ACR. However, continuous cloud cover during the two-week period following the *Puerto Rican* oil spill prevented its use in this study.

In summary, the oil spilled by the *Puerto Rican* experienced a sudden and dramatic reversal in its trajectory on or about 5 November 1984, which can only partially be explained by local wind drift. The behavior of this reversal was surge-like and it is possible that it was related to the onset of the Davidson Current. The strongest argument for the onset of the Davidson Current arises from the SST data acquired at the Farallon Islands during the period of the *Puerto Rican* oil spill. These data revealed a significant (approximately 2·0°C) systematic increase that is consistent with the expected advective change in local surface temperature that may have indicated the onset of the Davidson Current in the Gulf of the Farallones. However, as discussed, other explanations are also possible.

Finally, with the exception of the 5 November event, wind drift was the single most important factor in determining the history of oil movement during this spill, a result consistent with a number of other oil-spill studies. The mean-flow component was significant and most likely representative owing to the number of independent sources that provided estimates that were in close agreement. The tidal contribution was undoubtedly small but could have been important if the oil spill had occurred closer to the Golden Gate. The addition of further model components would have been inconsistent with the reductionist-modeling approach adopted here and dictated by the limited observational data that were available.

ACKNOWLEDGMENTS

REFERENCES

Bratkovich, A., Bernstein, R. L., Chelton, D. B. & Kosro, P. M. (1991). The Central California Coastal Circulation Study: Program overview and representative results. In Southern California Bight Physical Oceanography, ed. C. D. Winant. Minerals Management Service, US Dept. Interior, pp. 91–109.

Chelton, D. B., Bratkovich, A., Bernstein, R. L. & Kosro, P. M. (1988). Poleward flow off Central California during the spring and summer of 1981 and 1984. *J. Geophys. Res.*, **93**, 10 604–20.

Churgin, J. & Halminski, S. J. (1974). Temperature, salinity, oxygen and phosphates in waters off United States, Vol. III: Eastern North Pacific, US Dept of Commerce, NOAA, Environmental Data Service.

Clarke, A. J. & Battisti, D. S. (1981). The effect of continental shelves on tides. Deep Sea Res., **28**, 665–82.

Conomos, T. J. (1975). Movement of spilled oil as predicted by estuarine nontidal drift. Limmology and Oceanography, **20**, 159–73.

Crosby, D. S., Breaker, L. C. & Gemmill, W. H. (1993). A proposed definition for vector correlation in geophysics: theory and application, *J. Atmos. and Oceanic. Tech.*, (in press).

Galt, J. A. (1984). Trajectory analysis and modeling support for the *Puerto Rican* oil spill. Unpublished manuscript.

Galt, J. A. (1988). Personal communication.

Godin, G. (1972). The Analysis of Tides, University of Toronto Press, Toronto, Canada.

Grose, P. L. & Mattson, J. S. (Eds) (1977). The *Argo Merchant* oil spill: a preliminary scientific report, US Dept. of Commerce, NOAA, Washington, DC, USA.

Herz, M. J. & Kopec, D. (1985). Analysis of the *Puerto Rican* tanker incident Recommendations for future oil spill response capability, Technical Report No. 5, The Paul F. Romberg Tiburon Center for Environmental Studies, Calif., 120 pp.

Hess, W. N. (ed.) (1979). The *AMOCO Cadiz* oil spill: a preliminary scientific report. US Dept. of Commerce, NOAA/ERA Special Report.

Hickey, B. M. (1979). The California Current System-hypotheses and facts, *Progress in Oceanography*, **8**, 191–279.

Hoult, D. P. (1972). Oil spreading on the sea. In *Annual Reviews of Fluid Mechanics*, ed. M. Van Dyke, W. G. Vincenti & J. F. Wehausen, **4**, 341–68.

Huang, N. E. (1979). On surface drift currents in the ocean, *J. Fluid Mech.*, **91**, 191–208.

Jeffreys, W. H. & Berger, J. O. (1992). Ockham's razor and Bayesian analysis. *American Scientist*, **80**, 64–72.

Jupp, P. E. & Mardia, K. V. (1980). A general correlation coefficient for directional data and related regression problems. *Biometrika*, **67**, 163–73.

Kundu, P. K., Allen, J. S. & Smith, R. L. (1975). Modal decomposition of the velocity field near the Oregon coast. *J. Phys. Oceanogr.*, **5**, 683–704.

Lentz, S. J. & Chapman, D. C. (1989). Seasonal differences in the current and temperature variability over the Northern California shelf during the Coastal Ocean Dynamics Experiment, *J. Geophys. Res.*, **94**, 12571–92.

Lissauer, I. and Welsh, P. (1978). Can oil spill movement be predicted? In *In the*

& Kosro, P. M. (1991). The
'rogram overview and repre-
Physical Oceanography, ed.
S Dept. Interior, pp. 91–109.
: Kosro, P. M. (1988). Pole-
ing and summer of 1981 and

, salinity, oxygen and phos-
tern North Pacific, US Dept
vice.

continental shelves on tides.

predicted by estuarine non-
159–73.

993). A proposed definition
l application, *J. Atmos. and*

ing support for the *Puerto*

of Toronto Press, Toronto,

Argo Merchant oil spill: a
nerce, NOAA, Washington,

'uerto Rican tanker incident
:apability, Technical Report
for Environmental Studies,

pill: a preliminary scientific
iecial Report.

stem-hypotheses and facts,

1 *Annual Reviews of Fluid*
J. F. Wehausen, **4**, 341–68.
e ocean, *J. Fluid Mech.*, **91**,

izor and Bayesian analysis.

elation coefficient for direc-
netrika, **67**, 163–73.
Modal decomposition of the
eanogr., **5**, 683–704.
ferences in the current and
alifornia shelf during the
s. Res., **94**, 12571–92.
nent be predicted? In *In the*

Wake of the Argo Merchant: a Symposium, Center for Ocean Management
Studies, University of Rhode Island, Providence, RI, USA.

Marmer, H. A. (1926). Coastal Currents Along the Pacific Coast of the United
States, Dept. of Commerce Special Publication No. 121, Government Printing
Office, Washington, DC, USA.

Murray, S. P. (1982). The effects of weather system, currents, and coastal
processes on major oil spill at sea. In *Pollutant Transfer and Transport in
the Sea*, Vol. II, ed. G. Kullenberg. CRC Press, Boca Raton, FL, USA.

Nelson, C. S. (1976). Seasonal variation in processes related to the California
Current. Unpublished manuscript.

Nelson, C. S. (1977). Wind stress and wind stress curl over the California Current,
NOAA Technical Report. NMFS SSRF-714, US Dept. of Commerce.

Pollack, A. M. & Stolzenbach, K. D. (1978). Crisis science: investigations in
response to the *Argo Merchant* oil spill. Sea Grant Program, M.I.T., Report
No. MITSG 78–8.

Reid, J. L., Roden, G. J. & Wyllie, J. G. (1958). Studies of the California Current
System, California Cooperative Oceanic Fish Investigation, Progress Report,
1 July 1956 to 1 January 1958. Marine Research Committee, California
Department of Fish and Game, Sacramento, California, USA. pp. 27–57.

Reisbig, R. L. & Alofs, D. L. *et al.* (1973). Measurements of oil spill drift caused
by the coupled parallel effects of winds and waves. *Mem. Soc. Roy. Sci.
Liege, 6 serie*, **6**, 65–75.

Rosenfeld, L. K. & Beardsley, R. C. (1987). Barotropic semidiurnal tidal currents
off Northern California during the Coastal Ocean Dynamics Experiment
(CODE). *J. Geophys. Res.*, **92**, 1721–32.

Schwartzberg, H. G. (1970). Spreading and movement of oil spills. Federal
Water Pollution Control Administration, US Dept. of Interior.

Schwartzlose, R. A. (1963). Nearshore currents of the western United States and
Baja California as measured by drift bottles. California Co-operative
Oceanic Fisheries Investigations Progress Report, 1 July 1960 to 6 June
1962, Marine Research Committee, California Department of Fish and
Game, Sacramento, California, USA, pp. 15–22.

Scripps Institution of Oceanography (1985). Surface water temperatures at
shore stations; United States west coast, SIO Reference 85-35, University of
California, Scripps Institution of Oceanography, La Jolla, California, USA.

Send, U., Beardsley, R. C. & Winant, C. D. (1987). Relaxation from upwelling
in the Coastal Ocean Dynamics Experiment. *J. Geophys. Res.*, **92**, 1683–98.

Smith, C. L. (1974). Determination of the leeway of oil slicks, Dept. of Trans-
portation, US Coast Guard Report. No. CG-D-60-75.

Smith, J. E. (1968). *'Torrey Canyon' Pollution and Marine Life*. Cambridge
University Press, New York, NY, USA.

Stolzenbach, K. D., Madsen, O. S., Adams, E. E., Pollack, A. M. & Cooper, C.
K. (1977). A review and evaluation of basic techniques for predicting the
behavior of surface oil slicks, M.I.T. Sea Grant Program, Report No.
MITSG 77–8.

Strub, P. T., Allen, J. S., Huyer, A., Smith, R. L. & Beardsley, R. C. (1987).
Seasonal cycles of currents, temperatures, winds, and sea level over the
Northeast Pacific. *J. Geophys. Res.*, **92**, 1507–26.

Strub, P. T. & James, C. (1988). Atmospheric conditions during the spring and

fall transitions in the coastal ocean off the western United States. *J. Geophys. Res.*, **93**, 15561–84.

Tomczak, G. (1964). Investigations with drift cards to determine the influence of the wind on surface currents. *Oceanographie*, **10**, 129–39.

US Dept. of Commerce (1973). Tidal current charts for San Francisco Bay, NOAA National Ocean Survey, Rockville, MD, USA.

US Dept. of Commerce (1984*a*). Tidal current tables, Pacific Coast of North America and Asia, NOAA National Ocean Survey, Rockville, MD, USA.

US Dept. of Commerce (1984*b*). Oceanographic Monthly Summary, NOAA National Weather Service and National Environmental Satellite, Data, and Information Service, Washington, DC, USA.

Winant, C. D., Beardsley, R. C. & Davis, R. E. (1987). Moored wind, temperature and current observations made during Coastal Ocean Dynamics Experiments 1 and 2 over the Northern California continental shelf and upper slope. *J. Geophys. Res.*, **92**, 1569–604.

Wyllie, J. G. (1966). Geostropic flow of the California Current at the surface and at 200 m, California Co-operative Oceanic Fisheries Investigations Atlas No. 4, Marine Research Committee, California Department of Fish and Game, Sacramento, California, USA.